Global Advanced Research Journal of Physical and Applied Sciences (GARJPAS) Vol. 1(1) pp. 012-031, November, 2012
Available online http://garj.org/garjmbs/index.htm

Full Length Research Paper

Geo-electrical resistivity and groundwater flow modells for characterization of a hardrock aquifer system

K'Orowe, M.O.*[1], Nyadawa, M.O.[1], Singh, V.S.[2] Rangarajan, R[2]

[1]Jomo Kenyatta University of Agriculture and Technology, P.O Box 62000, Nairobi, Kenya
[2]National Geophysical Research Institute, Uppal Road, Hyderabad 500-007, India

Accepted 16 October 2012

In the present study, focus is on evaluation of the utilization of geo-electrically derived hydraulic parameters and processes in groundwater flow modelling. Aquifer parameters and processes data, namely, formation factor, transmissivity and natural recharge at some locations are correlated linearly with geo-electrical resistivity of a hard rock aquifer in the Jangaon sub-watershed, Hyderabad, India. Petrophysical relations have been used to transform resistivity distribution into transmissivity and natural recharge distribution. The coherence of geo-electrically derived parameters has been tested by integrating them into a groundwater flow model. This was performed using MODFLOW codes during one hydrologic cycle within two time periods; time period one coinciding with the rainy season, when there is recharge to the aquifer with no pumping occurring at observation boreholes. During the second time period, dry conditions prevail, hence there is no recharge but observation boreholes are pumped. At the end of the simulation period, simulated groundwater water heads were compared with the observed hydraulic heads and a close match between the observed hydraulic heads and simulated heads has shown the reliability of geo-electrical data as a means of estimation of hydraulic parameters.

Keywords: Hydrogeological characterization, Geo-electrical data, groundwater flow model

INTRODUCTION

Successful groundwater flow modelling can result in an improved characterization and conceptualization of a hydrogeological system. Transmissivity (T), porosity (ϕ), Natural recharge and Specific yield are all commonly applied hydrogeologic parameters in groundwater flow modelling (Fitts, 2002). Improvements in modelling of groundwater flow will only come about with improved methods of determinations of these parameters. Direct methods would generally require drilling boreholes which provides accurate information at a point. However sparse field hydrogeological observations and/or lack of relevant in situ test results, frequently, hinder regional characterization processes.

In view of these constraints, a geo-electrical method for parameter estimation would be an attractive complimentary/alternative approach. Geo-electrical methods provide densely sampled information. The technique measures the electrical properties of an earth material which are related to hydraulic parameters. The procedure provides measurements indirectly and minimally invasively and can be controlled through appropriate field survey procedure.

The potential benefits of geophysical data in hydrogeological site characterization have been stated in numerous studies (Chen et al, 2001; Hubbard and Rubin, 2005, Butler, 2005 etc). The challenge however is to

*Corresponding author Email: modondi@yahoo.com

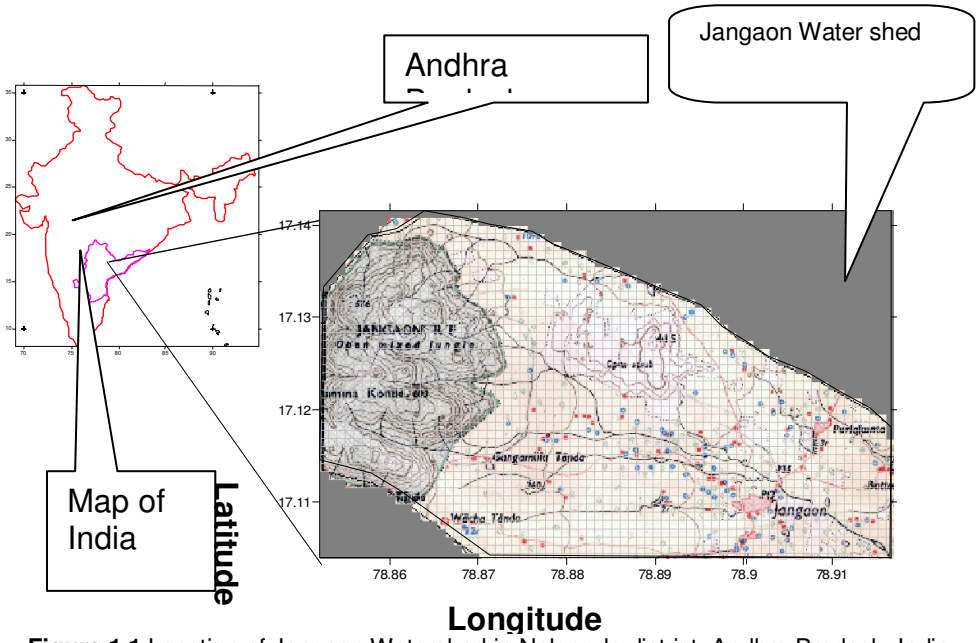

Figure 1.1 Location of Jangaon Watershed in Nalgonda district, Andhra Pradesh, India

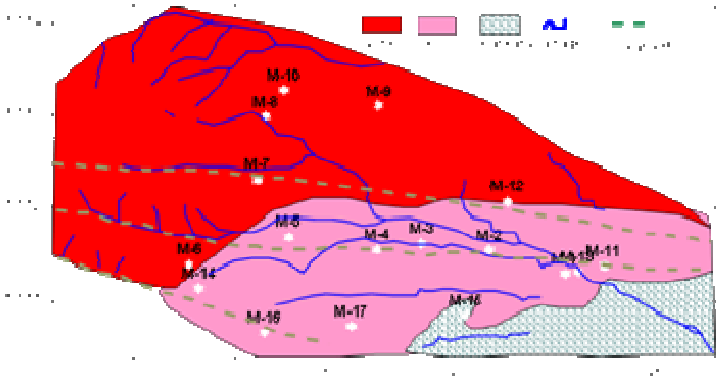

Figure 1.2 Geological map of the Jangaon sub-watershed

relate the geophysical observations and hydrogeological properties in an appropriate way.

In order to integrate hydrological and geophysical data, formulas that describe the relations between these properties are commonly used, and can be calibrated as site-specific conversions (Alumbaugh et al, 2002) or based on theoretical or general empirical models (Slater et al, 2002 ; Singha and Georelick, 2005 ; Singh, 2005). Converting geophysical data to hydrologic data using these formulas present some difficulties, in that the theories used to generate the relations are not able to fully capture conditions at the field scale.

The uncertainties and non-uniqueness of the relations have led researchers to try various techniques for incorporating geophysical property estimates into hydrogeology. McKenna and Poeter, (1995); Dietrich et al., (1998) correlated site specific geophysical data with collocated point hydrogeological data, Yeh et al, (2002) and Ramirez et al, (2005) considered stochastic methods, such as co-simulation and co-krigging frameworks.

Regardless of the fact that the geophysical data utilised for the case studies mentioned are different, it has been recognised that there is no universally acceptable petrophysical models for converting geophysical data to hydro geological attributes, partly due to the scale and resolution disparity between hydrological and geophysical measurements (Ezzedine et al, 1999). In this study, a

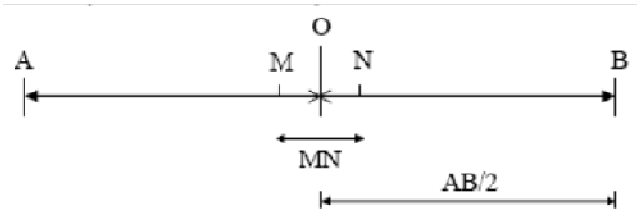

Figure 2.1 Schlumberger array configurations

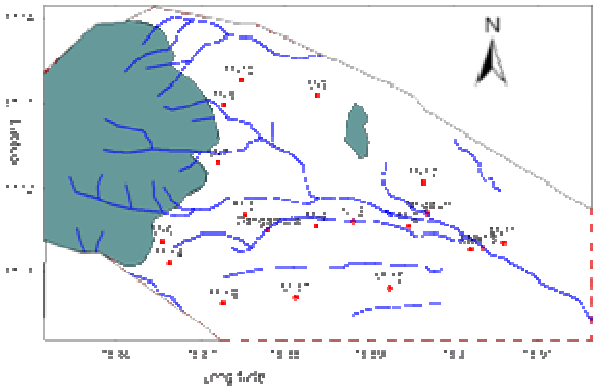

Figure 2.2: Location of Electrical sounding stations

Tables 2.1: Interpreted mean layer Resistivities and Thickness

STATION	ρ_1	ρ_2	ρ_3	ρ_4	h_1	h_2	h_3	Fittng errors
M-1	19.41	67.48	178.23	21238.96	0.35	6.76	13.46	4.1
M-2	47.79	36.43	163.09	3233.29	1.9	5.63	25.03	3.4
M-3	37.10	49.32	82.94	1095.27	0.8	6.00	15.55	3.5
M-4	285.03	28.08	209.15	11296.32	0.22	24.13	9.99	6.3
M-5	12.88	30.08	187.86	1100.87	0.53	23.12	10.64	4.6
M-6	23.17	43.69	13.97	5481.07	2.51	5.41	7.17	3.9
M-7	25.09	35.09	91.41	796.69	3.48	4.24	19.47	3.8
M-8	20.10	36.77	212.25	755.53	2.18	6.28	9.37	2.5
M-9	31.82	82.71	102239.59	-	0.25	8.48	-	6.1
M-10	38.48	86.84	24.53	13842.60	1.73	11.48	11.34	4.9
M-11	28.73	116.04	170.10	6483.81	1.08	21.50	8.00	2.6
M-12	35.77	196.08	4391.58	-	0.40	6.15	-	4.9
M-13	29.53	171.52	240.47	36824.02	1.44	7.34	4.94	2.8
M-14	26.29	189.77	27.03	1695.86	1.14	2.16	34.59	2.8
M-15	8.90	33.23	368.03	-	0.36	7.29	-	3.5
M-16	16.89	51.29	163.60	2025.59	9.62	31.01	24.84	9.0
M-17	44.23	14.72	95.83	1964.9	4.3	12.9	10.8	5.7

methodology has been developed that integrates groundwater resistivity data, formation bulk geo-resistivity parameter and depth models as an additional effort to improve on the characterization of aquifer parameters and processes. A theoretical linear relation developed between aquifer Transmissivity and formation factor (Korowe et al., 2011) has been used.

In order to validate the accuracy and coherence of the geo-electrical derived parameters, these parameters have been used as inputs in a groundwater flow model for a case study in the Jangaon sub-watershed, Hyderabad, Andhra Pradesh, India.

Recharge rates may be estimated from artificial tracer techniques. The artificial tracer techniques use tritium tracers. The technique of applying the tritium tracer in natural recharge estimation is described as the tritium injection method (Zimmermann et al, 1967a, b, Munnich, 1968a, b). This method assumes a piston flow model for movement of water infiltrating the vadose zone. The piston flow model has been verified in laboratory

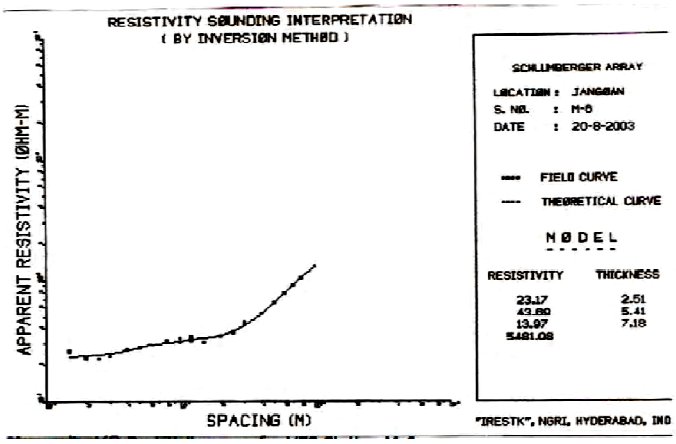

Figure 2.3. Resistivity curve for VES Station M-6

Plate 1 Exposed abandoned well near Ves-station M-3.

experiments, using mathematical models (Sharma et al, 1985; Rao and Jain, 1995), and in field conditions through multiple tritium injection experiments (Rangaranjan, 1997). The field and laboratory procedure adopted for measurement of spot recharge and a case study for measurement of natural recharge in a watershed is described in detail by Rangarajan et al, (2000).

Description of the study Area

The Jangaon sub-watershed, falls under the greater Waipalli watershed. It has an area of 28 km^2 and is situated about 80 km to the west of Hyderabad, Andhra Pradesh, India. It lies between longitudes 78.84^0 E and 79.92^0 E and latitudes 17.10^0 N and 17.14^0 N (Figure 1). Semi-arid climatic conditions prevail in the area, with minimum and maximum temperature of 22^{0}C and 44^{0}C, respectively. It has also been established that irrespective of the amount of rainfall, mainly from the Southwest monsoon in the months of June -December, annual rainfall is highly varieble from year to year. Drought conditions prevail for more than four months in any given year with April and May being the driest months.

Geology

Geology of the study area consists of granites of Achaean group of rocks represented by older group of rocks and peninsular gneissic complex. The older rocks include hornblende schist, pink and porphyritic granite gneisses, pink granites and injection of quartz, pegmatites and epidote veins represent biotitic schist and amphibolites while peninsular gneissic complex. Dolerites mark the last phase of igneous activity in the area and they cut across all the above rocks.
The geological map is shown in figure 1.2

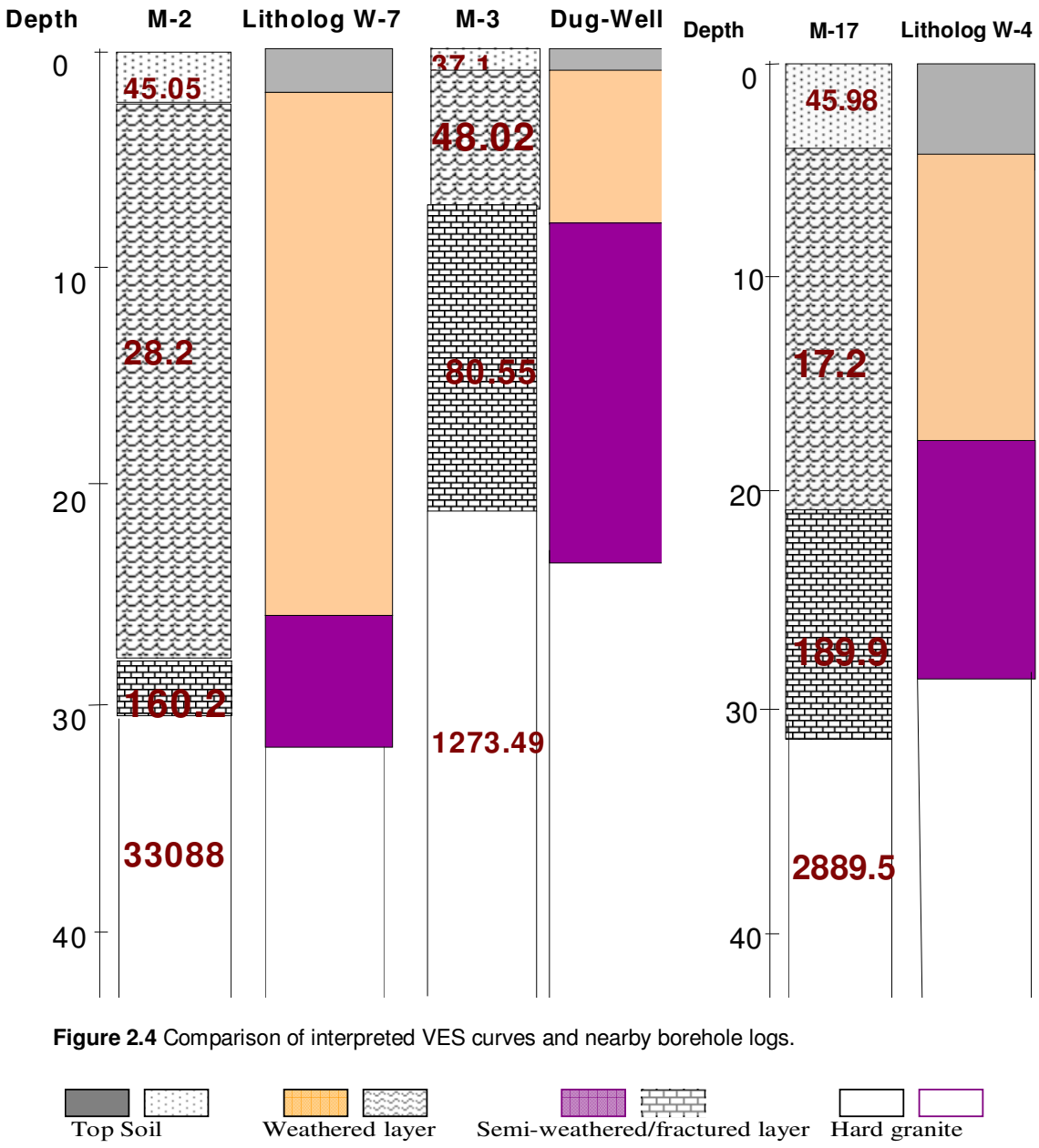

Figure 2.4 Comparison of interpreted VES curves and nearby borehole logs.

METHODOLOGY

Groundwater flow models simulation require proper site characterisation involving estimates and distribution of aquifer properties and processes, subsurface extent and thickness of an aquifer system. In this paper, these elements have been achieved by integrating physical and geo-electrical methods which are traditionally handled as separate endeavours. Towards this end estimates have been made of aquifer thickness and extent, hydraulic conductivity, natural recharge, porosity fraction and specific yield of the aquifer.

Apparent resistivity

A profile of apparent resistivity values across an area can be developed by carrying out an electrical resistivity sounding method of data collection utilising four electrodes. In doing this, current is introduced into the ground through two electrodes, A, source and B, sink, respectively. The potential difference is measured between the electrodes M and N as shown in figure 2.1 .A quantity referred to as the apparent resistivity (ρ_a) is then obtained. The variation of apparent resistivity with change in electrode spacing and position will give the

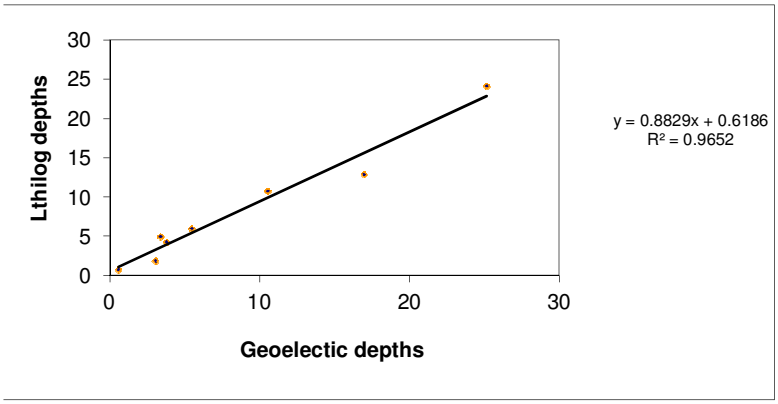

Figure 2.5 Correlation between resistivity sounding derived thicknesses and lithologs at VES stations M-2, M-3 and M-17.

Table 2.2. of depth to basement at VES-Stations

STATION	h_1	h_2	h_3	Depth-to Basement
M-1	0.35	6.76	13.46	20.57
M-2	1.9	5.63	25.03	32.56
M-3	0.8	6.00	15.55	22.35
M-4	0.22	24.13	9.99	34.34
M-5	0.53	23.12	10.64	34.29
M-6	2.51	5.41	7.17	15.09
M-7	3.48	4.24	19.47	27.19
M-8	2.18	6.28	9.37	17.83
M-9	0.25	8.48	-	8.73
M-10	1.73	11.48	11.34	24.55
M-11	1.08	21.50	8.00	30.58
M-12	0.40	6.15	-	6.55
M-13	1.44	7.34	4.94	13.72
M-14	1.14	2.16	34.59	37.89
M-15	0.36	7.29	-	7.65
M-16	9.62	31.01	24.84	65.47
M-17	4.3	12.9	10.8	28.0

information about subsurface layering.

The value of apparent resistivity is obtained from equation 1

$$\rho_a = \frac{G\Delta V}{I}, Where, G = \frac{2\pi}{\frac{1}{AM} - \frac{1}{AN} - \frac{1}{BM} - \frac{1}{BN}} \quad (1)$$

During interpretation, resistivity inversion scheme has been done using a computer code GENRES by Verma and Pantulu (1990). The program incorporates a linear filter described by Ghosh (1971). The root mean square (rms) error between observed and computed VES data was maintained at less 10% while computing the resistivity and thickness of the aquifer at various observation points. Figure2.2 shows the locations of the VES stations. Table 2.1 is a summary of interpreted mean layer resistivities and thickness while figure 2.3 is a typical resistivty curve of the area.

Geo-electrical depth model Characterization

Correlations identify subsurface formations from resistivity sounding values at the sites where borehole data are not available. Figure 2.4 shows the geoelectrical profiles and borehole logs at the VES stations M-2, M-17 and M-3.

Depth of layers observed in boreholes and abandoned wells located near VES stations M-2, M-3 and M-17 correlate very well with depth of layers derived from geo-

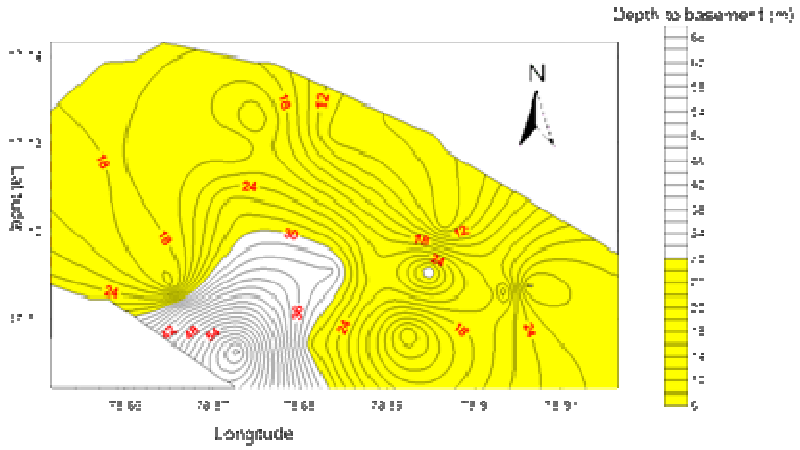

Figure 2.6 Distribution of the depth to basement.

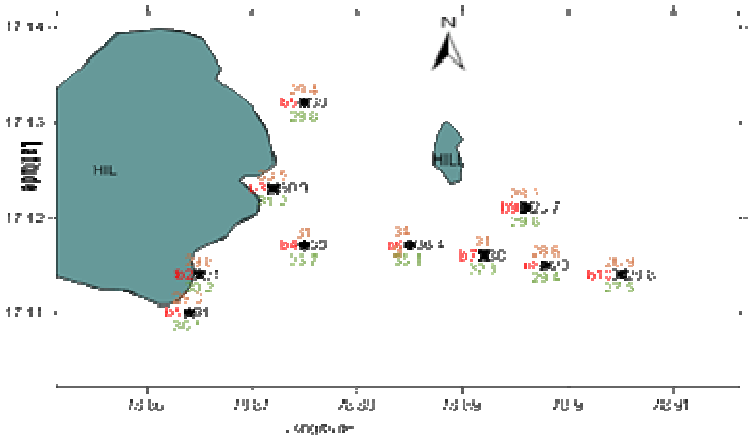

Figure 2.7 Static water levels at observation boreholes during one hydrologic cycle

KEY for Figure 2.7

Black labels are pre-monsoon heads (start of hydrologic cycle)

Brown labels are post-monsoon heads

Green labels are pre-monsoon heads (end of hydrologic cycle)

electrical inversion results shown in Figure 2.5. Electrical resistivity data is therefore capable of producing accurate stratigraphic results in terms of the thickness of the layers; hence the general thickness subsurface structure should be adequately provided for, by the geo-electrical sounding data itself in all the other areas where there are no collocated lithological data.

In Figure 2.6 shallower bedrock is indicated towards the north of the study area. The deepest portion is at the southern portion of the study area, showing values of more than 60 meters deep. This comes as a result of gradient relief in this direction, which favors accumulation of debris and water that initiates weathering. In general, depth to basement increases from north to south.

Geo-electrical resistivity model characterization

The resistivity models inferred from the inversion results of this area have both four and three layers stratigraphy. A simple section comprising of three regolith-weathering

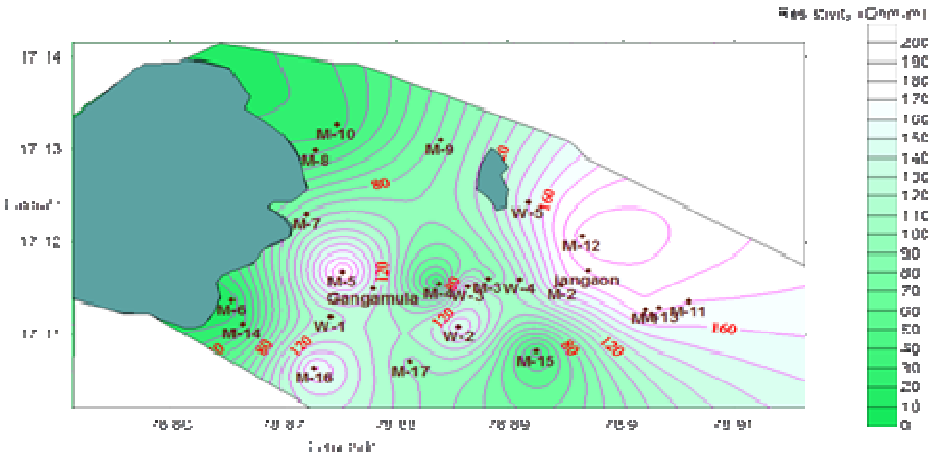

Figure 2.8 The distribution of the resistivity of the saturated aquifer.
Note; VES stations are marked M-1, M-2, M-3……..e.t.c, Pump test boreholes

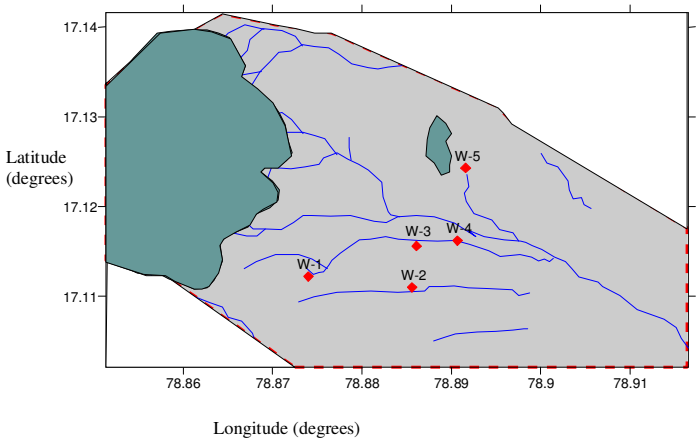

Figure2.9 Location of Pumping test boreholes; Jangaon sub-watershed

units has been suggested using the weathering units suggested by Gangadhara (1992).

Resistivity values have therefore been grouped into four units. The simplified regolith-weathering units thus assumed for the Jangaon sub-watershed are;

1) Weathered rock (10 – 50 Ohm-m)
2) Semi-weathered rock (50-120 Ohm-m)
3) Fractured (120 –300 Ohm-m)
4) Basement rock has resistivities greater than 300 Ohm-m

From the grouping, the aquifer of the region may be found within the semi-weathered and within the fractured rock. It should be noted that there is no sharp boundary between formations in any environment, hence the grouping does not strictly demarcate the boundaries, and allowance has been made for overlaps between layers. The Jangaon sub-watershed has in many instances developed dry weathered zones as seen from the many abandoned shallow wells and deep static water levels. The static water levels during the pre-monsoon seasons for the beginning of the hydrologic cycle and the end of the cycle range from 23 m to 38 m and 26.86 m to 34.94 m respectively (Figure 2.7).

As a result, saturated aquifers will occur at the bottom of the weathered layer and in portions of fractured portion of the hard rock. The weathered layer, which would contain groundwater under water table conditions, has, in most cases, been desaturated because of semi-arid conditions and poor recharge. This, in, effect has rendered the fracture aquifers to be unconfined. For purposes of determining the extent of saturated aquifer, the layer overlying the basement has been considered. Figure 2.8 is the distribution of resistivity for the inferred aquifer.

The aquifer is taken as the layer in contact with the resistive basement. The resistivity of this layer varies from resistivity 10 ohm-m to 200 ohm-m.

Transmissivity estimation from geo-electrical data.

A close analogy exists when groundwater and electric

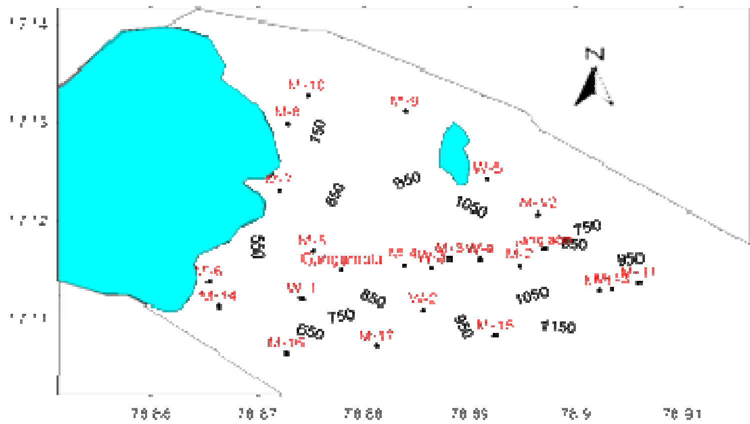

Figure 2.10 Distribution of kriged specific conductance (μmhos cm^{-1})

Table 2.3 Electrical and hydraulic parameters at the pumping test boreholes.

Borehole	T (m^2/day)	ρ (Ohm-m)	EC (μMho/cm)	$\rho_f = \frac{10000}{EC}$ (Ohm-m)	F_a
W-1	44.2	112.2	992	10.08	11.13
W-2	24.7	156.5	895	11.17	14.01
W-3	45.7	133.1	853	11.72	11.36
W-4	37.6	112.2	1033	9.68	11.59
W-5	35.1	150.2	835	11.97	12.55

The specific conductance values in column four (4) of table 2.4 are obtained from the distribution of kriged specific conductance in figure 2.10.

current flow are considered in an aquifer. There flow depends on the respective potential gradients. While groundwater flow depends on the hydraulic conductivity (K) of the formation, electric current flow depends on the electrical conductivity (σ) of the formation. The ions flow through the same paths as water thus the electrical conductivity and hydraulic conductivity of aquifer should be influenced by same factors. In hard rock environments, it is electrolytic conduction which is important and therefore the most important influencing factor is the water available in the secondary porosity of the aquifer medium. This means that Darcy's law of groundwater flow and Ohms law for current flow operate on a common water medium. By inference, therefore, the two flows are related.

Bernabe and Revil (1995) obtained the formula for pore scale network electrical conductivity and hydraulic permeability, respectively as;

$$c = c_f \frac{\sum_{cracks\ tubes}^{n} V_p(n)|\nabla \psi(n)|^2}{V|\nabla \Psi|^2} + c_s \frac{\sum_{cracks,\ tubes}^{n} A_p(n)|\nabla \psi(n)|^2}{V|\nabla \Psi|^2} \qquad (2)$$

$$k = \frac{\sum_{cracks} \frac{V_p(n)^3}{3A_p(n)^2}|\nabla \varphi(n)|^2 + \sum_{tubes} \frac{V_p(n)^3}{2A_p(n)^2}|\nabla \varphi(n)|^2}{V|\nabla \Phi|^2} \qquad (3)$$

where, c_f is conductivity of fluid filling the pores, c_s, conductivity of pore surface, V_p (n) is pore volume, A_p (n) is pore surface area, ΔΨ (n) is potential gradient across pores, Δφ (n) is head gradient across pores, n is the number of pores through which both electrical and hydraulic flow occurs, and the summation is done over these pores. In this study, it is stipulated that the sum of energies dissipated for both electrical and hydraulic parameters at the network level must equal the energy dissipated at the field level due to energy conservation. K'Orowe et al.,(2011) used this assumption, together with the bond shrinkage model ideas of Wong *et al.* (1984), in up-scaling intrinsic pore relationship to field based petrophysical relationship between the formation factor(F_a) and transmissivity (T) for the Jangaon sub-watershed arrive at a relationship used in this study of the form ;

Table2.4. Calculated hydraulic conductivity parameters.

Station	ρ (Ohm-m)	b_e (m)	EC (µMho/cm)	$\rho_f = \frac{10000}{EC} F_a = \frac{\rho}{\rho_f}$ (Ohm-m)		T (m^2/day)	K=T/ b_e (m/day)
M-1	178.23	13.46	1125	8.89	20.05	11.07	0.822
M-2	163.09	26.03	1155	8.66	18.83	12.95	0.498
M-3	82.94	15.55	1265	7.91	10.49	55.92	3.596
M-4	209.15	9.99	1049	9.53	21.95	8.83	0.884
M-5	187.86	10.64	801	12.48	15.05	22.68	2.132
M-7	91.41	19.47	687	14.56	6.28	201.66	10.357
M-8	212.25	9.37	692	14.45	14.69	24.10	2.572
M-9	82.71	8.48	823	12.15	6.81	164.68	19.420
M-11	170.10	8.00	1037	9.64	17.65	15.23	1.904
M-12	196.08	6.15	834	11.99	16.35	18.44	2.998
M-13	240.47	4.04	1098	9.11	26.40	5.57	1.379
M-16	163.6	24.84	601	16.64	9.83	65.79	2.649
M-17	95.83	10.8	918	10.9	8.8	86.76	8.033

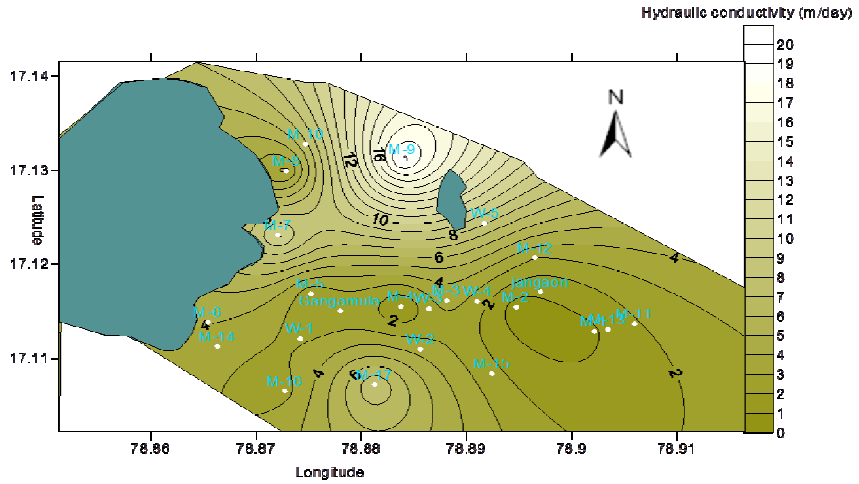

Figure 2.11 Distribution of Kriged estimates of hydraulic conductivity

ln (T (m^2/day)) =-2.5ln F_a +9.9 (4)

together with the value of cementation factor established for the area of $m_\phi = 3.4$), the equation forms the basis of the relationship for generating transmissivity and porosity fraction from apparent resistivity data used in this paper and presented in table 2.4.

.

Aquifer test results

Groundwater drawdown and recovery at the monitoring wells during quifer test provided a consistent assesment of transmissivity of the aquifer.

For this study, individual fractures were not explicitly treated in the model. The heterogeneity of the hard rock system has been modeled as an equivalent porous medium. Thus the primary and secondary porosity and the transmissivity distribution are replaced with a continuous porous medium having equivalent hydraulic properties. The Jacob's method has been used in conjunction with the Neumann *et al.,* (1984) method for interpretation of the pumping tests. So, while the Cooper and Jacob's method (1946) addresses the porous nature of the medium, Neumann's method takes care of the heterogeneity inherent in hard rocks. Pumping test was done on the boreholes in locations W-1, W-2, W-3, W-4, and W-5 Figure 2.9. The bulk resistivity data in column 3 of table

2.3 are obtained from the distribution of the resistivity of the saturated aquifer figure 2.8

Estimation of formation resistivity factor

The formation factor F_a is the formation property (independent of fluid) that determines the ability for an electrical current to flow through pore space.

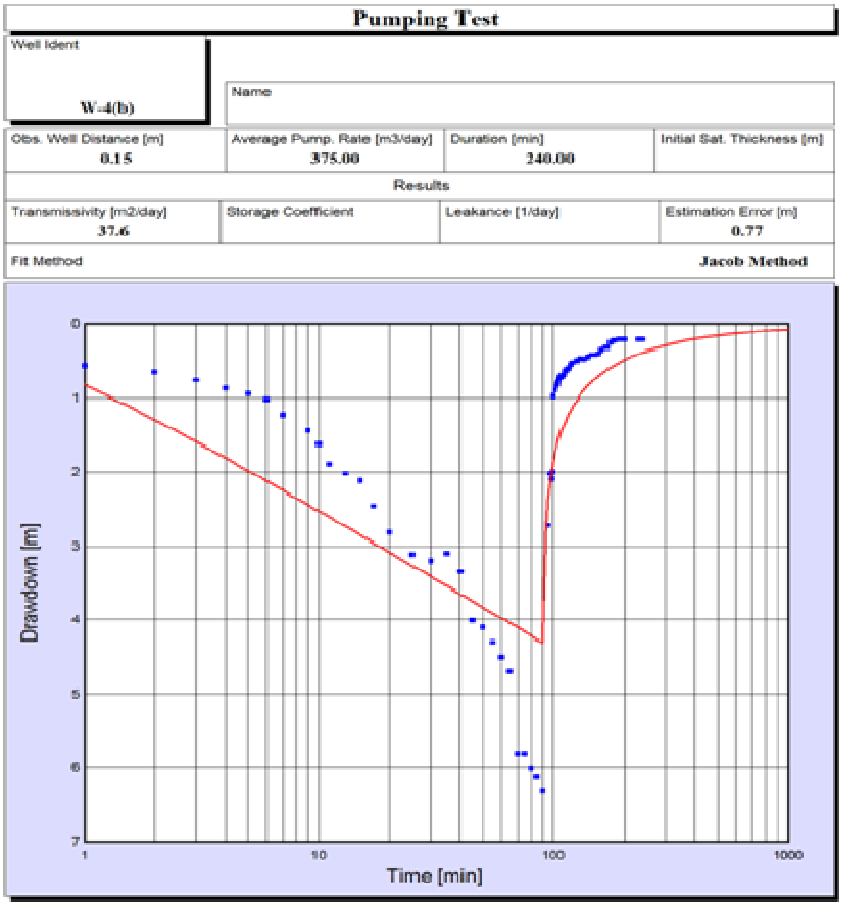

Figure 2.12. Pumping test data for borehole W-4 after adjustment for anisotropy

Table 2.5 Porosity estimates.

Station	Formation factor (F_a)	Calculated porosity fraction $\phi = \left(\frac{1}{F_a}\right)^{\frac{1}{3.4}}$
M-1	20.05	**0.41**
M-2	18.83	**0.42**
M-3	10.49	**0.50**
M-4	21.95	**0.40**
M-5	15.05	**0.45**
M-6	2.5	**0.76**
M-7	6.28	**0.58**
M-8	14.69	**0.45**
M-9	6.81	**0.57**
M-10	1.72	**0.85**
M-11	17.64	**0.43**
M-12	16.35	**0.44**
M-13	26.40	**0.38**
M-14	1.91	**0.83**
M-15	3.64	**0.68**
M-16	9.83	**0.51**
M-17	6.11	**0.59**

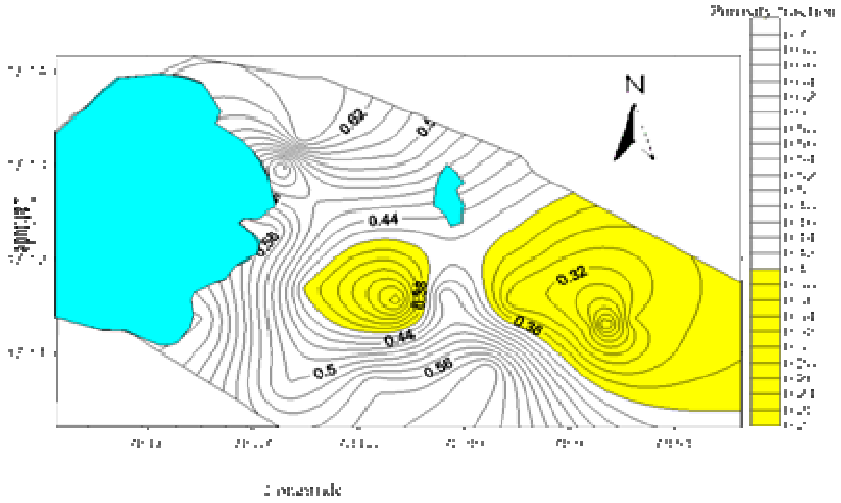

Figure 2.13 Kriged estimates of porosity fraction

Table 2.6 Evaporation rates at specific sites.

Longitude	Latitude	Depth below surface (z) (m)	$EVAP^{dry}$ $(71.9z^{-1.49})$ mm/yr
78.864	17.110	30.1	0.45
78.865	17.114	30.2	0.45
78.875	17.117	33.7	0.38
78.872	17.123	31.2	0.43
78.875	17.132	29.8	0.46
78.885	17.117	35.1	0.36
78.892	17.116	32.2	0.41
78.896	17.121	29.8	0.46
78.898	17.115	29.4	0.47
78.905	17.114	27.5	0.52

From Table 2.6, by taking the average value of EVAP in column four, the average value is determined as 0.44 mm/yr.

Table 2.7 Groundwater balance components during dry period

RF^{dry} (m/yr)	Q^{dry} (m/yr)	$EVAP^{dry}$ (m/yr)	HIN^{dry} -$HOUT_{DRY}$	Δh^{dry} (m)	S_p
0.0053	0.0485	0.00044	0	-2.7	0.016

Ruiz and Kobr (1989) developed an empirical relationship between the resistivity of a fully brine saturated system of insulating grains given as follows.

$\rho = F_a\rho_w$, where

ρ: electric resistivity of the saturated rock, obtained from surface resistivity surveys

ρ_w :is the electric resistivity of water in the rock.

The requisite formation facors at the pumping wells are indicated in column 6 of table 2.3

Groundwater resistivities

Groundwater resistivities in the area were determined from measurements of specific conductance of groundwater at wells and boreholes distributed in the area, figure 2.10.

A conductivity-meter was dipped into the water sample instrument and a reading of specific conductance in units

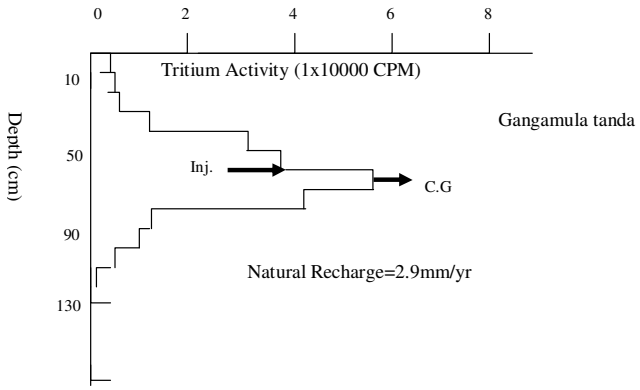

Figure 2.14. Variation of tritium activity with depth at Gangamula tanda.

Table2.8 Longitudinal conductance, transverse resistance, recharges and Sand/Gravel contents at injection sites

Station	Longitude (degrees)	Latitude (degree)	S	T_r	$\left(\rho_t = \sqrt{\frac{T_r}{S}}\right)$	Recharge (mm/yr)	Sand/Gravel (%)
Jangaon	78.90	17.12	0.053	261.2	43.2	15.9	42.4
Gangamula	78.88	17.12	0.12	102.4	26.0	2.9	38.0
Rangaipally	79.41	18.34	0.05	80	40	72	48.0
Manzurnaga	79.51	18.25	0.06	165	52.4	100	43.0
Karkapally	79.83	18.33	0.14	350	50	101	49.0
Paripally	79.36	18.30	0.03	146	69.8	132	55.0

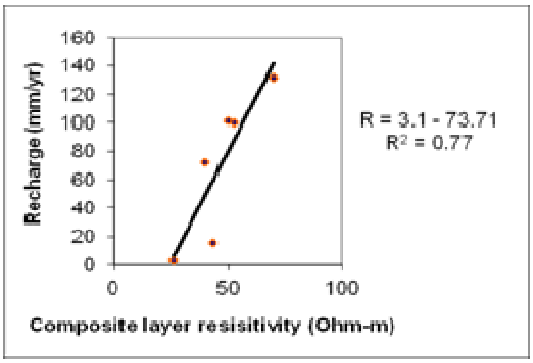

Figure 2.15 Plots of recharge versus composite layer resistivity.

of µMho/cm recorded for calculation of the resistivity values of the saturating water. The resistivity value of the saturating water was obtained by taking the reciprocal of groundwater specific conductance. To get the value in units of ohm-meters is equivalent to dividing the specific conductance values by a factor of 10,000.

Estimating porosity

Archie's (1942) empirical formula relates the composite resistivity of the medium to the resistivity of the formation water as follows;

Estimating porosity from geo-electrical data involves the use of the well-known Archie's law (Archie, 1942). $\phi = \left(\frac{1}{F_a}\right)^m$, where m is the cementation factor of the rock, for the area of study, m = 3.4 (K'Orowe et al.,2011).Porosities at each VES station was then calculated. The calculated values are shown in Table 2.5 column three, while kriged distribution is shown in Figure 2.13.

Table 2.9 Calculated recharges Values.

VES-Stations	ρ_1	ρ_2	h_1	h_2	T	S	ρ_t	Recharge (R) (3.1 ρ_t -73.71)
M-1	19.41	67.48	0.928	6.587	157.83	0.08	44.4	63.9
M-2	47.79	36.43	2.296	5.589	134.7	0.07	43.9	62.4
M-3	37.10	49.32	0.800	6.00	138.2	0.07	44.4	63.9
M-4	285.03	28.08	0.813	21.923	293.1	0.08	60.5	113.8
M-5	12.88	30.08	1.087	21.031	76.3	0.15	22.6	-
M-6	23.17	43.69	2.835	6.949	82.1	0.13	25.1	4.1
M-7	25.09	35.09	3.691	4.362	75.3	0.15	22.4	-
M-8	20.10	36.77	2.544	6.163	67.9	0.14	22.3	-
M-9	31.82	82.71	0.840	8.106	205.4	0.05	64.1	125
M-10	38.48	86.84	2.146	10.754	156.7	0.07	47.3	72.9
M-11	28.73	116.04	1.572	19.602	210.9	0.07	54.9	96.5
M-12	35.77	196.08	0.972	6.049	432.4	0.04	104	248.7
M-13	29.53	171.52	1.891	7.099	246.1	0.07	59.3	110.1
M-14	26.29	189.77	1.14	2.16	386.4	0.05	87.9	198.8
M-15	8.90	33.23	0.937	7.055	76.9	0.17	21.3	-
M-16	16.89	51.29	9.112	21.808	50.67	0.18	16.8	-
M-17	44.23	14.72	4.3	10.8	132.7	0.07	43.5	61.1

Recharge values from VES stations M-16, M-15, M-7, M-8 and M-5 were omitted in the Kriging of recharge measurements as they produce negative recharge values, probably because of very little recharge at these sites.

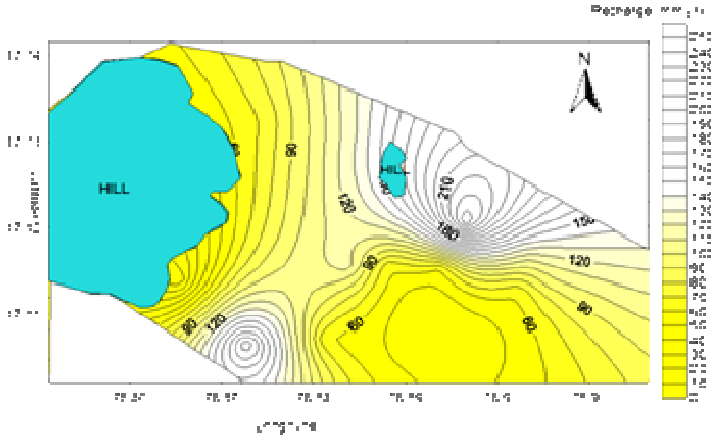

Figure 2.16 Distribution of Natural Recharge using ordinary Kriging.

Estimation of Specific Yield

In trying to estimate the specific yield of an aquifer using the groundwater balance method, the values of the following groundwater budget components are evaluated; Change in water levels (Δh), Water pumping flow rate (Q), return flow (RF) and Evaporation (EVAP).

Change in water levels (Δh)

The groundwater balance method requires that the peizometric level over the entire basin be known. This was achieved by using observation boreholes. Water levels were measured three times, at beginning of rainy season (season 1), near the end of the rainy season (season 2) and at the end of the next dry season (season 3) within a hydrological cycle. The value of Δh^{dry} has been taken as the maximum water level fluctuation between seasons 2 and season 3 static water levels.

Pumping flow rate (Q)

The ground water draft for Jangaon was recorded as 135.85 million-hectare meters (135.85 Mham) per year by the Central Groundwater Board of India (2003) from the Basin wide draft show this is equivalent to a draft of

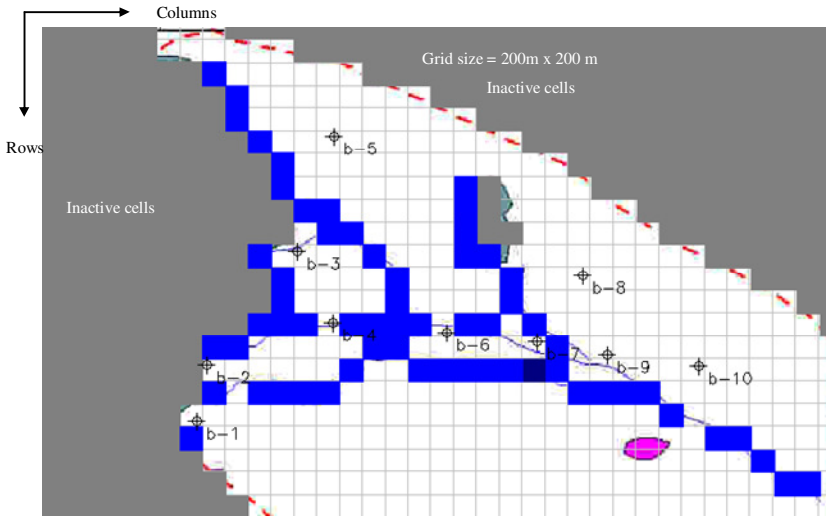

Figure 2.17.Simulation domains in grid map format.
Note: observation boreholes are marked; b-1, b-2, b-3.....etc

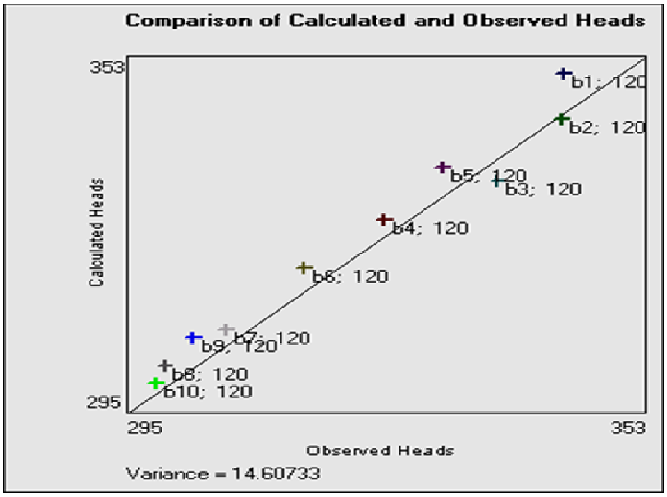

Figure 3.1a: Scatter plot for transient state simulation model (period 1, time step 6)

1358.5 km^3.

Return flow from irrigation (RF)

The bulk of the pumped water in the area is used for irrigation of the paddy fields. Most of this returns to the aquifer by direct infiltration in the irrigated lands. This is represented as: RF=C*Q, where C, is the return coefficient (0<C<1) and Q is the pumping flow. Return coefficient for paddy fields is different from other crops. The global return coefficient is therefore weighted by the partition of crops as expressed in equation 5.32.

$$A*C=A_{RICE}*C_{RICE}+A_{OTHER}*C_{OTHER} \quad (5)$$

where A, is the total irrigated surface, A_{RICE} is the surface area of irrigated paddy fields, $A_{OTHER,}$ area of other irrigated crops, C_{RICE} is return coefficient in paddy fields and C_{OTHER} is the return coefficient of other crops.

Establishing return coefficients of each crop is not easy to assess, however, in granite areas such as that found in the study area. The coefficient for paddy fields has been evaluated as 0.60 (APGWD, 1977). For other crops, the proposed coefficient is C_{OTHER} =0.20 (CGWB, 1998). The total area under groundwater irrigation (A) is 429.79 hectares, A_{RICE} is 77.7 hectares, and A_{OTHER} is 8.09

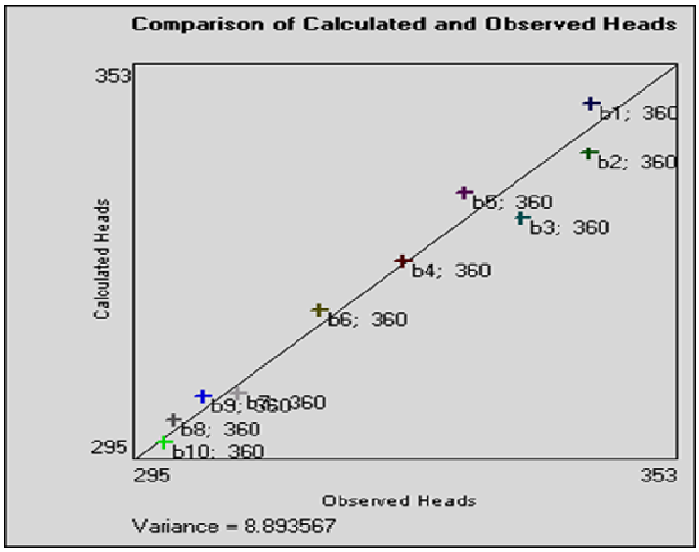

Figure 3.1b: Scatter plot for transient state simulation model (period 2, time step 12

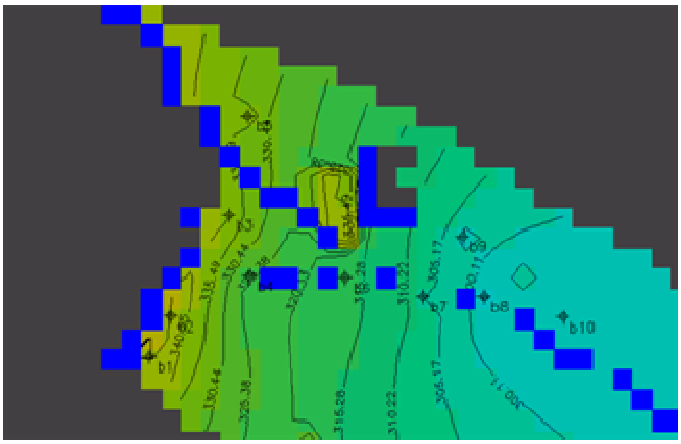

Figure 3.2 Initial ground water heads (m) distribution

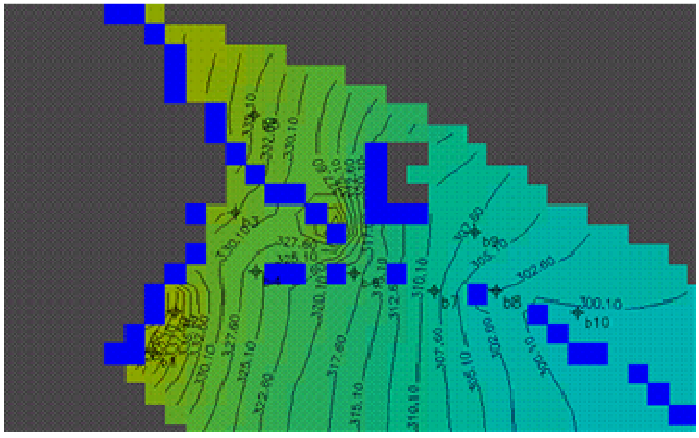

Figure 3.3a Ground water heads distribution (m) Period 1 time step 6

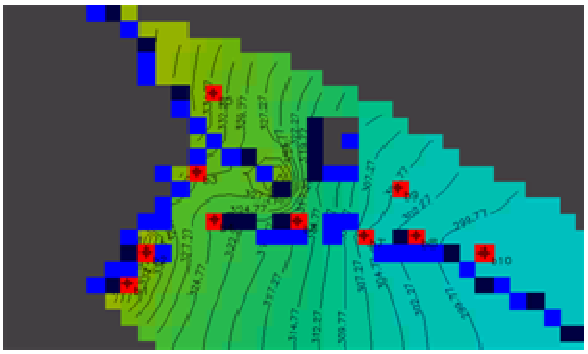

Figure 3.3b Ground water heads distribution (m) Period 2 time step 12

Table 3.1 Observed and Simulated hydraulic heads

OBSERVATION WELL	POST-MONSOON, HEADS Observed (m)	Simulated (m)	Residual (%)	PRE-MONSOON, HEAD Observed (m)	Simulated (m)	Residual (%)
b1	345.6	350.3	-1.5	344.8	347.2	-0.7
b2	344.8	342.8	0.6	344.4	340.0	1.3
b3	340.5	333.0	2.2	337.8	330.5	2.2
b4	321.0	326.4	-1.6	323.3	324.1	-0.2
b5	338.9	335.0	1.2	338.5	334.2	1.3
b6	316.3	318.7	-0.8	316.1	316.8	-0.2
b7	305.0	308.5	-1.1	303.7	304.5	- 0.3
b8	294.5	302.6	-0.3	295.8	300.6	-1.6
b9	296.6	307.3	-3.6	293.0	304.2	-3.8
b10	300.0	299.8	0.1	299.4	297.4	0.7

hectares according to CGWB, (2003). Substituting the values A (429.79 hectares); A_{RICE} (77.7 hectares); C_{RICE} (0.60); A_{OTHER} (8.09 hectares) and C_{OTHER} (0.20) into equation 5, the global return coefficient, C is found to be 0.11.

Return flow (RF) is the product of global return coefficient and the total draft of the sub-water shed, which gives a value of 149.4 km^3.

Evaporation (EVAP)

The depth of water table below the surface during the dry season has been taken to coincide with those measured at the end of the hydrologic cycle.

From Table 2.6, by taking the average value of EVAP in column four, the average value is determined as 0.44 mm/yr.

Specific Yield (Sp)

The groundwater balance components used in calculating specific yield are listed in table 2.7

From Table 2.7, the specific yield is obtained by substitution of the balance components

whence, $S_p = \dfrac{0.0053 - 0.0485 - 0.00044}{-2.7} = 0.016$

Estimation 0f Natural Recharge

In order to develop site-specific relationship between geo-electrical resistivity data and natural recharge, collocated values of geo-electrical data and tritium injection data were prepared for correlation. Correlating the composite layer resistivity of the top 3 meter layer formations with recharge estimates from tritium injection data developed the relationship. The relationship is meant to provide a way of estimating natural recharge from geo-electrical data.

Tritium injection data at seven sites (Jangaon, Gangamula tanda and Wacha tanda, Rangapally, Manzurnagar, Karkapally and Paripalli) within the Jangaon sub-watershed and in the adjacent Lower manor basin, with different geomorphologic units and soil types were considered. Recharge was estimated by monitoring the vertical displacement of the injected tritium. A typical plot as in figure 2.14 shows a peak indicating position of

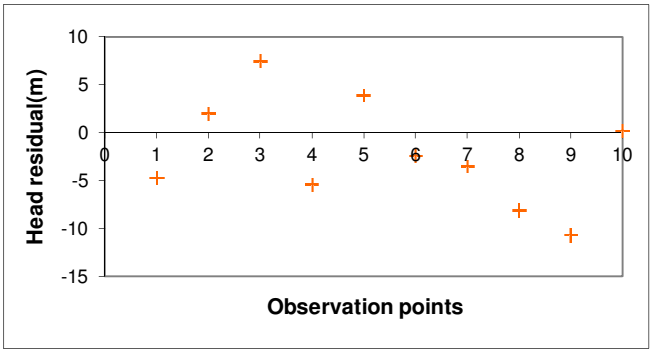

Figure 3.4a Residuals from comparison of measured and computed heads at calibration targets during transient simulation period 1 time step 6. The x-axis shows the observation points (i.e. boreholes b-1, b-2 b-3. …b-10)

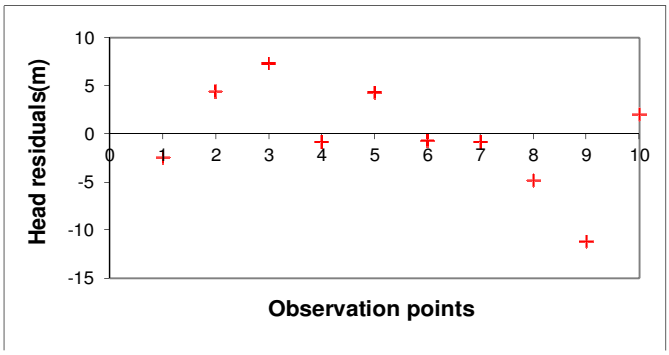

Figure 3.4 b Residuals from comparison of measured and computed heads at calibration targets during transient simulation period 2 time step 12.

the tracer during its displacement in tritium activity versus depth plot. The field and laboratory procedure adopted for measurement of spot recharge and a case study for measurement of natural recharge in a watershed is described in detail by Rangarajan and Athavale, (2000).

Composite layer resistivity and Recharge relation

Within the study area, consideration of soil-texture has therefore resulted in direct relationship between recharge and composite layer resistivity. 'Composite layer resisistivity' values $\left(\rho_t = \sqrt{\frac{T_r}{S}}\right)$ plotted against recharge, where T_r and S are transverse resistance and longitudinal conductance respectively and fitting a straight line to the data, provides a linear relationship (Figure 2.15),

The correlation between recharge and composite layer resistivity is given by equation (6)

R= 3.1 ρ_t -73.71 (6)

This is an empirical relationship and for purposes of this study, it is referred to as the site-specific geo-electrical model of recharge. The last column of table 2.9 shows calculated recharge values at specific VES stations. Krigged estimates of recharge are shown in figure 2.16

Integration of Proposed Geo-Electric Models of Aquifer Flow Process In Groundwater Flow Computation.

The simulation of groundwater flow requires the hydrogeological characterization of the site, which requires the establishment of subsurface extent and thickness of aquifers, hydrologic boundaries, hydraulic properties of the aquifers, a description of the distribution of hydraulic head throughout the modelled area for steady-state conditions and transient conditions, distribution and magnitude of groundwater recharge and stresses. The outputs from the model simulations are the hydraulic heads which are in equilibrium with the hydrogeological for the modelled area. In this study, a numerical groundwater flow model has been used. The approximations require that the model domain and time

during simulation be discretized (figure 2.15). In this discretization process, the model domain was represented by a network of grid cells and the length of simulation time was divided into stress periods, which are in turn divided into time steps. The length of stress periods and time steps are relevant only for transient state simulation.

The computer code chosen for this study is the processing MODFLOW (PMWIN version 5.1), developed by Chiang and Kinzelbach,(1998)..

The input data utilised, namely the extent and thickness of aquifers, hydraulic conductivity , effective porosity and natural recharge have been obtained from geo-electrical models, while specific yield, has been obtained from groundwater balance method.by recording the quantity of groundwater produced per unit time. The initial heads were set equal to the interpolated groundwater elevation, and were kept constant in the general head boundary cells during simulations. Terrain elevations were interpolated from the digitised contour maps by using spherical variograms.

Model Simulation

The model was calibrated under transient conditions over one hydrologic cycle under the following conditions;

i) Transient state conditions during the rainy season when there is recharge and pumping from the wells are not expected.

ii) After eight months of pumping with no recharge during the dry season

A no-flow boundary condition is realized by setting the flux as zero (Anderson and Woessner, 1992). No-flow boundaries have been assigned to the west of the region (Figure 2.17) as there exist a massive granite hill. At the Northern end of the study area a no-flow boundary has been conceptualized because there is change in the drainage pattern meaning that there is a groundwater flow divide along the edges of the hills. A constant flux condition was used to simulate groundwater flow into the modeled area due to check dams erected along the bases of these hills. The other boundary condition was that of aerial recharge and pumpages. Regular finite grids of $200m^2$ were used for the model.

During the rainy season, the river courses present as ephemeral rivers, which flow for some time within a year. Since surface water channels usually have direct or indirect effects on the groundwater system, they may create changes of water pressure in the aquifer that may modify flow rates and directions. Because of this, these values of influx to the flow domain were halved along the water channels away from the hills to reflect the short duration these channels are full of water. The transient calibration was carried out for one hydrologic cycle, given that heads data were available for only the period. Parameters are assigned to each node in the grid, and then model runs are made to match the calibration target.

ANALYSIS AND DISCUSSION

In carrying out calibration of the groundwater flow model, field measured heads are compared against simulated heads. Initial heads distribution is shown in figure 3.2. Figures 3.3a and 3.3b shows distribution of groundwater heads Period 1 time step 6 and Period 2 time step 12 respectively. The red grids indicate the wells being pumped. The ground water draft for Jangaon was recorded as 135.85 million-hectare meters (135.85 Mham) per year by the Central Groundwater Board of India (2003) from the Basin wide draft. This is equivalent to a draft of 1358.5 km^3 and has been distributed equally among the ten pumping wells. A graphical comparison between measured and computed heads is shown in Figures 3.1a and 3.1b. The degree of match between observed and computed heads, after convergence has been achieved, is compared using the value of the variance. If there is exact agreement between measurement and simulation, all points should lie on a 45^o line. The narrower the area of scatter, the better is the match. The closer the heads fall on the straight line, the better the 'goodness-of-fit'. The mismatch between computed and observed water heads at places may be attributed mainly to errors during interpolation of input parameters. The mismatches that occur near the river course (marked blue in figure 2.17) may be due to the sudden change in conductivity values between the riverbed and the adjacent hard rocks. Good correlation between calculated and observed heads is noticed for the end of the simulation period, period 2 time step 12 (Figure 3.1b). The difference between simulated and actual field groundwater heads (residuals) is shown as percentages during period 1 time step 6 and also during period 2 time step 12 (Table 3.1).At most of the observation points, simulated heads are noted to be larger than measured heads. If for example, the head observed in a well is a perfect measurement, a difference between observed and simulated head may result because the simulated head represents the average head over a volume of material with average properties. If the observation is not at a nodal point in the computer model, the nodal values are interpolated to obtain the simulated value. This is one of the possible errors introduced into the model simulated head values. Table 3.1 shows the observed and simulated heads for a single hydrologic cycle. It is observed that the residual percentage difference between values of observed heads and simulated heads for the post monsoon period, corresponding to period one time step six is in the range -3.6% and 2.2% while the pre-monsoon period corresponding to period two time step twelve has a value in the range -2.2% and -3.8%. The simulated heads closely match the observed heads. A plot showing

residuals at observation boreholes (calibration targets) are shown in Figure 3.4a and Figure 3.4b. A plot of this format is useful in showing the 'goodness-of-fit' at each observation borehole.

CONCLUSION

Integration of the geo-electrically derived hydraulic parameters and processes into groundwater flow model has shown that this indirect modeling approach produces simulated groundwater heads which are very close to those obtained by direct observation. For this case, model errors from residual hydraulic heads are less than 10% at all observation boreholes, which is within acceptable limits. Scatter plots of simulated heads versus measured heads at the end of simulation time have weighted variances at values of 8.89, a value indicative of the goodness fit between simulated and observed hydraulic heads. This again shows coherence between input parameters and output parameters into the flow domain. The coherence observed between geo-electrically derived input parameters and processes and outputs as represented by simulated heads, has demonstrated that geo-electrical techniques provide an alternative method for acquiring hydraulic parameters and processes data in order to adequately characterize flow in hard rock aquifers.

REFERENCES

Andhra pradesh groundwater department (1997) 'Studies on hydrologic parameters of groundwater recharge in water balance computations, Andhra Pradesh', *Government of Andhra Pradesh Groundwater Department, Hyderabad, Research series* 6, 151

Alumbaugh DL, Chang PY, Paprocki L, Brainard JR, Glass RJ, Rautman CA (2002) 'Estimating moisture contents in the vadose zone using cross-borehole ground penetrating radar: A study of accuracy and repeatability' *Water Resources Research,* 38, 1309.

Anderson MP, Woessner WW (1992). 'Applied Groundwater modeling: Simulation of and Advective Transport'. *Academic Press, San Diego.*

Archie G (1942) 'The electrical resistivity Log as an aid in determining some reservoir characteristics', *Trans- American Institute of mineral metrology',* 146, 54-62

Bernabe Y, Revil A (1995). 'Pore-scale heterogeneity, energy dissipation and the transport properties of rocks', *Geophysical Research. Letters,* 22 (12), 1529-1532.

Butler JJ Jr, (2005). 'Hydrogeological methods for estimation of spatial variations in hydraulic conductivity', *Hydrogeophysics, edited by Y.Rubin and S.S. Hubbard, Springer, Netherlands, 23*-58

Central groundwater board of India (1998). 'Detailed guidelines for implementing the groundwater estimation methodology', *Central Groundwater Board, Ministry of Water resources, Government of India*

Central groundwater board of India (2003). 'Occurrence, Genesis and Control Strategies of Fluoride, Waipalli Watershed, Nalgonda District Andhra-Pradesh, India', *Central Groundwater Board, Ministry of Water resources, Government of India*

Chen J, Hubbard S, Rubin Y (2001). 'Estimating the hydraulic conductivity at the South Oyster Site from geophysical tomographic
data using Bayesian techniques based on the normal linear regression model', *Water Resources Research,* 37(6): 1603-1613.

Chiang WH, Kinzelbach W (1998). 'Aquifer Simulation Model for Windows-Groundwater flow and transport modeling, an integrated program', *Gebruder Borntraeger Berlin, Stuttgart, ISBN 3-443-010393.*

Cooper HH, Jacob CE (1946). 'A generalized graphical method for evaluating formation constants and summarizing well field history', *Transaction American Geophysical Union* 27*, 526-534.*

Dietrtch PT, Whittaker, Teutsch G (1998). 'An integrated hydrogeophysical approach to subsurface characterization', *GQ 98 Conference, Tubngen, Federal Republic of Germany, (Luvain): International Association of Hydrological Sciences,* 513-519.

Ezzedine S, Rubin Y, Chen J (1999). 'Bayesian method for hydrogeological site characterization using borehole and geophysical survey data: theory and application to the Lawrence Livermore National Laboratory Superfund site', *Water Resources Research,* 35 (9) *2671-2683*.

Fitts CR (2002). 'Groundwater Science'*, Elsever publications, The Netherlands*, 167-175

Gangadhara TR (1992). 'Groundwater exploration techniques', *Lecture notes, National Geophysical Research Institute.*

Ghosh DP (1971). 'The application of linear filter theory to the direct interpretation of geoelectrical resistivity soundings', *Geophysics. Prospect,* 19, 192-217.

Hubbard SS, Rubin Y (2005). 'Hydrogeophysics, in Hydrogeophysics', *edited by Y. Rubin and S.S., Hubbard, Springer*.

Korowe MO, Nyadawa MO, Singh VS, Ratnakar D (2011). 'Hydrogeophysical parameter estimation for aquifer characterization in hard rock environments: A case study from Jangaon sub-watershed, India', *Joournal of Oceanography and marine science, 2(3), 50-62*

Ramirez AL, Nation JJ, Hanley WG, Aines R, Glacer RE, Sengupta SK, Dyer KM, Hickling TL, Daily WD (2005). 'Stochastic inversion of electrical resistivity changes using a Markov Chain Monte Carlo Approach', *Journal of Geophysical Research. 110:BO2101, DOI: 10:1029/2004JBOO3449*.

Rangarajan R, Athavale RN (2000). 'Annual replenishable groundwater potential of India-an estimate based on injected tritium studies', *Journal of Hydrology,* 234, 38-53.

Rangarajan R (1997). 'Natural recharge evaluation in selected basins of semiarid India using injected tritium', *PhD thesis, Osmania University, Hyderabad, 180.*

Rao SM, Jain SK (1985). 'Tracer transport modeling for unsaturated zone. Effect of anion exclusion and immobile water', *Isotophenpraxis,* 21(12)*:* 433-438.

Ruiz J, Kobz M (1998). 'Metodos Geofisicos de Pozo'. *Tomo I. Editorial ENSPES, ISPJAE. Cindad de La Habana, Cuba*

Sharma ML, Hughes MW (1985). 'Groundwater recharges estimation using chloride, deuterium and oxygen-18 profiles in the deep coastal sands of Western Australia', *Journal of Hydrology,* 81(1-2), 93-109

Singh KP (2005). 'Nonlinear estimation of aquifer parameters from surficial resistivity measurements', *Journal of hydrology and Earth Science,* 2: 917-938.

Singha K, Gorelick SM (2005). 'Saline tracer visualized with electrical resistivity tomography: field scale moment analyses, *Water Resources Research*,
41, *WO5023, doi: 10.1029/2004WR003460.*

Slater L, Binley A, Versteg R, Cassiani G, Birken R, Sandberg S (2002). 'A 3D ERT study of solute transport in a large experimental tank', *Journal of Applied Geophysics,* 49: 211-229.

Verma SK, Pantulu KP (1990) 'Software for the interpretation of resistivity sounding data for groundwater exploration' *National Geophysical Research Institute, Hyderabad-INDIA.*

Yeh TC, Liu S, Glass J, Baker K, Brainard JR, Alumbaugh DL, Labreque D (2002).'A geostatistical based inverse model for electrical resistivity surveys and its application to vadose zone hydrology', *Water Resources Research*, 39 (3), 13-14.

Zimmermann U, Ehhalt D, Munnich KO (1967a). 'Soil water movement and evapotranspiration; changes in the isotope composition of the water', *In: Isotopes in Hydrology, IAEA, Vienna*, 567-586

Zimmermann U, Munnich KO, Roether W (1967b). '*Downward movement of soil moisture traced by means of hydrogen isotopes',* American Geophysical Union, Geophysics. Monogram, 11, 23-36